A Simple Model for Liquid or Amorphous Metals

J. Blétry

Institut Laue-Langevin, 156 X Centre de Tri, 38042 Grenoble Cédex

(Z. Naturforsch. **32 a**, 445–452 [1977]; received February 17, 1977)

The structure of liquid or amorphous metals is described by means of an harmonic approximation where atoms vibrate around the equilibrium positions of a random hard sphere network. This model depends on three parameters, of which the only adjustable one is the atomic vibration frequency, which is shown to be proportional to the Debye frequency of the corresponding crystalline phase. The atomic diameter is deduced from the position of the structure factor first peak and turns out to be equal to the Goldschmidt diameter. The packing fraction temperature variations are attributed to presence of a variable number of randomly distributed atomic holes and deduced from density measurements. Good agreement with experimental structure factor determinations is found for a wide variety of liquid metals.

Introduction

The simplest description of monoatomic liquid structure has been proposed by Bernal [1] and coworkers [2] who packed about ten thousand spheres together in dense random aggregates or "clusters". However, this geometrical model agrees poorly with experiment because it does not take into account atomic movements.

Much more satisfactory results have been obtained either by Monte Carlo (M.C.) [3] or molecular dynamics (M.D.) [4] calculations. Both methods, which are exact in the classical mechanics sense, are susceptible in practice to some limitations. They usually involve a small number of particles and it is therefore necessary to make an approximate extrapolation of the pair distribution function beyond the first few neighbour distances [5]. Furthermore, special analytical forms of the interatomic potential have been used which are suitable for rare gases but rather unrealistic in the liquid metal case [6, 7].

The aim of the model proposed in this paper is to take into account a larger class of potentials while keeping the simplicity and large particle number involved in geometrical theories. Thus, a dense random network of hard spheres is first built in which particle number and packing fraction effects are studied. The corresponding pair distribution function is then modified by means of a convolution equation which describes the softness of the potential within an harmonic approximation. The resulting structure factors and their temperature dependence are shown to fit the most recent accurate measurements in a wide variety of liquid metals.

Reprint requests to Dr. J. Blétry, Institut Laue-Langevin, 156 X Centre de Tri, *F-38042 Grenoble Cédex*, Frankreich.

1. Hard Sphere Model

1.1. Computer Algorithm

Since it is useful to pack together a large number of spheres N, the main time saving computing techniques are presented which allow the generation of a 15812 particle cluster.

First of all, cartesian geometry formulae are used which avoid the introduction of any fortran function except for one square root per atomic position calculation.

In order to locate the particles, the aggregate is enclosed in a cubic box divided into elementary cells with side $d/\sqrt{3}$, where d is the sphere diameter. Each cell can only accomodate one sphere center and is characterized by an occupation number which is either 0 or 1. If i, j, k are the cell indexes of a given particle, the cell indexes of its contact neighbours lie in the range $i+2>l>i-2$, $j+2>m>j-2$, $k+2>n>k-2$. This set of 125 cells form the so called "close neighbourhood" Ω_P of a particle P.

Starting from an initial triangular seed of three spheres in contact the cluster is grown by successive additions of new spheres in contact with three spheres of the same neighbourhood, according to the Sadoc et al.[8] "bump growing" process. Sphere overlaps are avoided by comparing the position of each eventual new particle E with those pertaining to the full cells of its close neighbourhood Ω_E.

1.2. Cluster Packing Fraction

A spherical shape is given to the cluster by adding the condition that the distance r_i between a particle and the center of the aggregate must be less than:

$$r_i < \frac{d}{2}\left(\frac{N_t}{\gamma_t}\right)^{1/3} = r_{\max}$$

where $\gamma_t = 0.65$ and N_t are respectively the desired packing fraction and particle number.

Inversely, assuming perfect sphericity, we deduce the cluster radius R from the mean distance of the particles to the center of this cluster, according to the relation:

$$R = \frac{4}{3} r_m = \frac{4}{3}\frac{1}{N}\sum_1^N r_i .$$

The derivation of the packing fraction γ which is the ratio of the N sphere volume to the cluster volume V:

$$\gamma = N \pi d^3 / 6 V$$

follows immediately. This true packing fraction is smaller than the desired one, because the desired particle number N_t cannot be reached with the present algorithm.

1.3. Calculation of the Pair Distribution Function

The pair distribution function is defined as the probability $P(r)$ of finding a particle at a distance r from another one, normalized in such a way that it tends to unity as r approaches infinity. In order to obtain $P(r)$ up to the maximum $r = 2R$ value with the best possible accuracy, this probability is deduced from the total number of particle pairs whose distance lies between r and $r + \mathrm{d}r$: $\mathrm{d}N(r)$. According to Fournet[9], one finds for a spherical aggregate:

$$\mathrm{d}N(r) = \frac{\pi^2}{6}(N/V)^2 r^2 (2R - r)^2 (4R + r) P(r)\,\mathrm{d}r$$
$$= \varrho^2 S(r) P(r)\,\mathrm{d}r \quad \text{for} \quad r < 2R \qquad (1)$$

where $\varrho = N/V$ is the number density
and $S(r) = (\pi^2/6) r^2 (2R - r)^2 (4R + r)$ is a geometrical factor.

However, our cluster exhibit diameter fluctuations of the order of 2 d and Eq. (1) may only be used up to $r \cong 2(R - d)$.

Furthermore, discrete $P(r)$ values are calculated with a constant step $\Delta r = r_{j+1} - r_j = 0.05\, d$ and they are limited in precision because the number of particle pairs in this interval $\Delta N(r)$ is finite. The mean square value of the corresponding statistical fluctuations is given by:

$$2\tau^2(r) = \frac{1}{n}\sum_1^n [P(r_{j+1}) - P(r_j)]^2 \cong \frac{2}{\Delta N(r)}$$
$$= \frac{2}{\varrho^2 S(r) P(r) \Delta r} \qquad (2)$$

with

$$r = \frac{1}{n}\sum_1^n r_j$$

and provided the conditions:

$$n \Delta r [\mathrm{d}P(r)/\mathrm{d}r] \ll P(r) \qquad (3)$$

and

$$\Delta r [\mathrm{d}P(r)/\mathrm{d}r] \ll \tau(r) \qquad (4)$$

are fulfilled. For large r values where $P(r)$ is almost always equal to 1, inequalities (3) and (4) are easily satisfied and a good order of magnitude for the expected relative precision of $P(r)$ is obtained around $r = R$ where:

$$\tau^2 \cong \frac{32}{15}\frac{R}{\Delta r} N^{-2} \qquad (5)$$

[see Tables (1) and (2)].

1.4. Structure Factor Calculation

The intensity scattered by a randomly oriented cluster is given by the Debye formula

$$I(K) = 1 + \frac{2}{N}\sum_{i, r_i = d}^{2 r_{\max}} \frac{\sin(K r_i)}{K r_i} \Delta N(r_i) \qquad (6)$$

where K is the modulus of the scattering vector. $I(K)$ may also be expressed as the sum of a small angle scattering term due to the finite size of the aggregate and an intrinsic structure factor $A(K)$ according to the Guinier relation[10]:

$$I(K) \cong N |\Phi(K)|^2 + A(K) \qquad (7)$$

where

$$\Phi(K) = 3\frac{\sin(KR) - KR\cos(KR)}{(KR)^3} \qquad (8)$$

is the Fourier transform of the spherical cluster form factor. The structure factor is deduced from the combination of Equations (6), (7) and (8). However, departures from sphericity produce spurious oscillations in $A(K)$ below $Kd \cong 2$.

The structure factor may also be calculated by means of the Zernike-Prins equation:

$$A(K) = 1 + \frac{N}{V}\int e^{i\mathbf{K}\mathbf{r}}[P(\mathbf{r}) - 1]\,\mathrm{d}_3 r$$

$$= 1 + \frac{6\gamma}{\pi d^3}\int_0^\infty \frac{\sin(K r)}{K r}\,[P(r) - 1]\,4\pi r^2\,\mathrm{d}r\,. \quad (9)$$

However, the $P(r)$ cut-off at large r again produces spurious $A(K)$ oscillations below $K d \cong 2$.

1.5. Sphere Diameter Influence

The effect of a particle diameter change on the pair distribution function and the structure factor corresponds to the simple equations:

$$\begin{cases} P_d(r) = P_{d_0}(r\,d_0/d) \\ A_d(K) = A_{d_0}(K\,d/d_0) \end{cases} \quad (10)$$

1.6. Particle Number Influence

Five clusters having between 1000 and 15812 particles and the same packing fraction $\gamma = 0.52$ were studied. Figure 1 shows that there is no change in $P(r)$ and $A(K)$ when increasing N except for the reduction of $P(r)$ statistical fluctuations which according to relation (5) decrease as $N^{-5/3}$ (see Table 1). Thus differences between random packing models arise mainly from packing fraction effects.

1.7. Packing Fraction Influence

The packing fraction is varied from $\gamma = 0.52$ down to $\gamma = 0.064$ by randomly removing 0 to 7000 particles from a 8000 particle cluster, a process which preserves its external shape. Under these conditions and according to its definition, $P(r)$ does not vary with γ. Nevertheless, $P(r)$'s statistical fluctuations decrease as does N^{-2} according to relation (5). (See Table and Figure 2.)

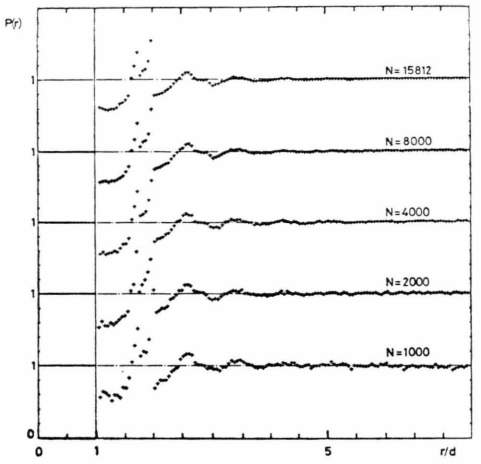

Fig. 1. Variation of the pair distribution function with the number of particles in the cluster.

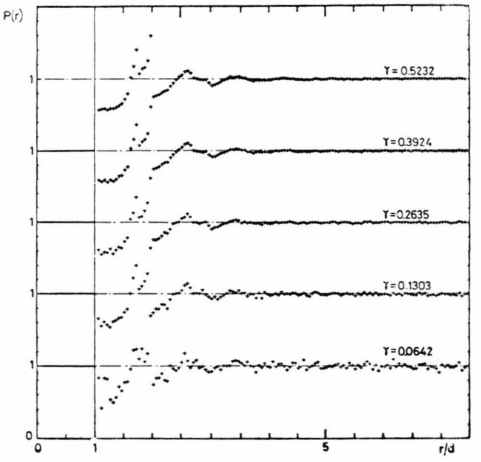

Fig. 2. Variation of the pair distribution function with the cluster packing fraction.

Table 1. Variation of $P(r)$ mean square fluctuations with the particle number.

N	1000	2000	4000	8000	15812
τ^2 calculated from Eq. (5)	$2.6\cdot10^{-4}$	$8.4\cdot10^{-5}$	$2.6\cdot10^{-5}$	$8.4\cdot10^{-6}$	$2.6\cdot10^{-6}$
τ^2 observed	$2.4\cdot10^{-4}$	$8.8\cdot10^{-5}$	$2.6\cdot10^{-5}$	$1.0\cdot10^{-5}$	$2.6\cdot10^{-6}$

Table 2. Variation of the $P(r)$ mean square fluctuations with the packing fraction.

γ	0.0642	0.130	0.263	0.328	0.392	0.456	0.523
τ^2 calculated from Eq. (5)	$5.0\cdot10^{-4}$	$1.3\cdot10^{-4}$	$3.3\cdot10^{-5}$	$2.1\cdot10^{-5}$	$1.5\cdot10^{-5}$	$1.1\cdot10^{-5}$	$8.4\cdot10^{-6}$
τ^2 observed	$5.0\cdot10^{-4}$	$1.5\cdot10^{-4}$	$3.6\cdot10^{-5}$	$1.5\cdot10^{-5}$	$1.4\cdot10^{-5}$	$1.5\cdot10^{-5}$	$1.0\cdot10^{-5}$

Table 3. $P(r)$ peak positions and intensities.

$P(r)$	1st max.	1st min.	2nd max.		2nd min.	3rd max.	3rd min.	4th min.	4th max.	5th max.	5th min.
Finney positions in d units	1	1.38	1.73	1.99	2.20	2.65	3.12	3.47	3.92	4.25	
Blétry positions in d units	1	1.275	1.725	1.975	2.08	2.63	3.03	3.43	3.88	4.30	4.70
Blétry $P(r)$ intensity		0.605	1.444	1.430	0.804	1.114	0.923	1.040	0.982	1.021	0.990

Table 4. $A(K)$ peak positions and intensities.

maximum and minimum positions in $1/d$ units	7.72	10.36	13.70	17.30	19.96	23.60	26.50	29.64	32.60	35.86	38.80
maximum and minimum $A(K)$ intensities	2.340	0.529	1.456	0.678	1.368	0.793	1.274	0.824	1.196	0.844	1.166

On the other hand, Table 3 shows that the extrema positions and intensities of our $P(r)$ curve agree fairly well with those reported by Finney [2] which correspond to a larger packing fraction $\gamma_F = 0.6366$. Beyond γ_F, it is uncertain whether atomic holes are still present in the structure. However the soft sphere model, which allows sphere overlaps, may lead to larger packing fractions while retaining almost the same structure. Thus, it should be safe to consider the pair distribution function $P_d^{HS}(r)$ independent of the packing fraction even for $\gamma > \gamma_F$. Its second peak, which is split into subpeaks at $r = 1.73\,d$ and $r = 1.98\,d$, as well as the asymmetry of the third and fourth peak are characteristic of the local fivefold symmetry which forbids periodicity. Beyond the sixth peak, $P_d^{HS}(r)$ oscillations become very weak although they still contribute to the integral involved in Equation (9).

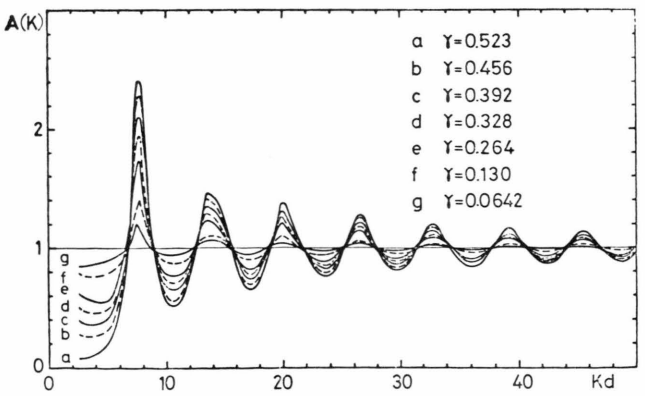

Fig. 3. Variation of the structure factor with the packing fraction.

For $\gamma < \gamma_F$, the structure factor varies linearly with γ according to the relation:

$$A_\gamma(K) = 1 + \frac{\gamma}{\gamma_F}\,[A_{\gamma_F}(K) - 1] \qquad (11)$$

and its first peak is situated at:

$$K_1 = 7.72/d \qquad (12)$$

(see Table 4 and Figure 3). For larger packing fractions, the linear relation (11) may be extrapolated in the K range where it leads to positive $A_\gamma(K)$ values, that is to say for $K < K_0$ where K_0 is defined by:

$$1 + (\gamma/\gamma_0)\,[A_{\gamma_0}(K_0) - 1] = 0\,. \qquad (13)$$

2. Harmonic Approximation

2.1. Discussion of the Approximation

The liquid or amorphous metal is represented by a set of identical and independent harmonic oscillators in thermodynamical equilibrium which vibrate around the random hard sphere network positions. This Einstein model is certainly a good approximation for amorphous metals where each atom has a well defined mean position. Furthermore, it is probably as justified as M.C. and M.D. theories in the liquid case, since our approximation is equivalent to the replacement of the true potential which has a minimum value $-V_0$ and a full width at half minimum $2W$ by a harmonic well with the same characteristics:

$$V_H(x, y, z) = -V_0 + (V_0/2W^2)\,[(x - x_0)^2 + (y - y_0)^2 + (z - z_0)^2]$$

On the other hand, the harmonic potential may represent a large variety of interactions since its relative width $\delta = 2W/r_0$ can be varied over a wide range starting from the hard sphere value $\delta = 0$. On the contrary, recent M.C. and M.D. calculations did not vary δ sufficiently enough to describe very soft interactions [7, 11, 12]. Finally it may be noted that our approach is very similar to the translator-oscillator description of Hicter et al.[13] with the difference that translators are neglected because they do not affect significantly the structure factor although they mainly contribute to diffusion processes.

2.2. Pair Distribution Function and Structure Factor Calculation

At a temperature T, the probability of finding an harmonic oscillator with mass m at a distance $\boldsymbol{r}$ from its equilibrium position is:

$$H(\boldsymbol{r}) = (2\pi\sigma^2)^{-3/2} \exp\{-r^2/2\sigma^2\}$$

where: (14)

$$\sigma^2 = \frac{\hbar}{2m\omega} \coth\left(\frac{\hbar\omega}{2kT}\right) \quad \text{and} \quad \omega = \sqrt{\frac{V_0}{mW^2}}.$$

Thus the static pair distribution function is now given by the convolution equation:

$$P_d^{\sigma}(\boldsymbol{r}) = \int P_d^{\mathrm{HS}}(\boldsymbol{r}-\boldsymbol{r}')\, G^{\sigma}(\boldsymbol{r}')\, d^3 r'$$

where:

$$G^{\sigma}(\boldsymbol{r}) = (4\pi\sigma^2)^{-3/2} \exp\{-r^2/4\sigma^2\}$$

has a variance $2\sigma^2$ since the two extremities of an atomic pair are moving. Figure 4 shows the overall broadening and damping of $P(r)$ oscillations with increasing σ, i. e. potential softness. In particular, the splitting of the $P(r)$ second peak disappears around $\sigma \cong 0.06\, d$.

By Fourier transforming $P_d^{\sigma}(r)$ one immediately obtains the soft sphere structure factor *

$$A_{d,\gamma}^{\sigma}(K) = 1 + \frac{N}{V} e^{-\sigma^2 K^2} \int e^{i\boldsymbol{K}\boldsymbol{r}} [P_{d,\gamma}^{\mathrm{HS}}(\boldsymbol{r}) - 1]\, d_3 r$$

$$= 1 + \frac{\gamma}{\gamma_0} e^{-\sigma^2 K^2} \left[A_{d_0,\gamma_0}^{\mathrm{HS}}\left(K\frac{d}{d_0}\right) - 1 \right] \quad \text{for } K > K_0. \tag{15}$$

A similar derivation of the Debye Waller factor may be used in the case of crystals.

* The corresponding program is available on request at ILL.

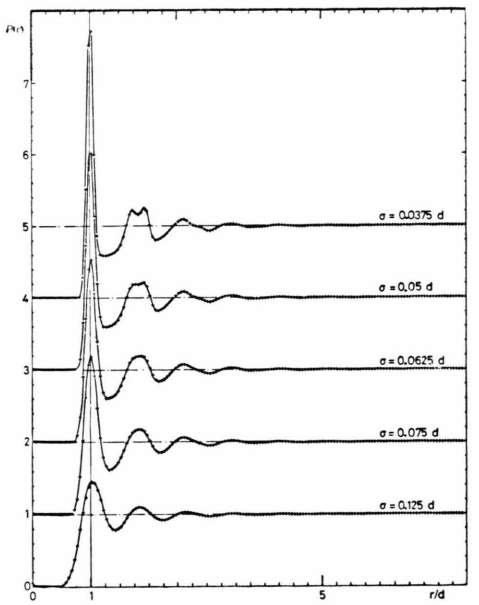

Fig. 4. Variation of the pair distribution function with the potential softness.

2.3. High Temperature Limit

In order to reach the high temperature regime $\hbar\omega \ll kT$ while still remaining within the harmonic approximation one must add the supplementary condition $kT \ll V_0$. This restriction leads to $V_0 \gg V_{\mathrm{L}} = \hbar^2/mW^2$ (where V_{L} is the localization energy in the potential well) and shows that the interaction potential should not be too hard, as in the liquid metal case [11]. With these conditions σ^2 reduces to:

$$\sigma^2 \cong kTW^2/V_0 = kT/m\omega^2. \tag{16}$$

3. Comparison with Experiment

3.1. Main Parameters

In order to check the validity of our model, we show that it can describe the structure of several liquid metals with different electronic structure as well as the temperature variations of the liquid rubidium structure factor which has been recently studied over a wide temperature range.

In order to fit these experimental data we only adjust the atomic vibration frequency $\nu = \omega/2\pi$ which turns out to be roughly one half of the Debye

Table 5. Comparison of model frequency and Debye frequency.

Metal	Cu	Zn	La	Rb
ν in 10^{12} s^{-1}	3.9	2.95	1.34	0.769
Debye frequency in 10^{12} s^{-1} from [24]	$6.34<\nu_D<7.13$	$4.17<\nu_D<6.36$	$2.75<\nu_D<3.17$	$1.21<\nu_D<1.77$

Table 6. Comparison of hard sphere diameter and Goldschmidt diameter.

Metal	Cu	Zn	La	Rb
d in Å	2.56	2.74	3.74	5.03
$d_{Goldschmidt}$ in Å from [25]	2.56	2.74	3.74	5.02

frequency ν_D of the corresponding crystalline phase for a wide variety of metals (see Table 5). This result which is in close agreement with Ruppersberg and Hicter finding [14] clearly shows the physical meaning of ω and suggests possible inelastic neutron scattering experiments on the liquid metals where accurate structure factor measurements are available.

The equivalent hard sphere diameter d is deduced from the position of the structure factor first peak near the melting point according to formula (12) and turns out to be equal to the Goldschmidt diameter within 2% precision for a wide variety of metals (see Table 6). This result provides new evidence for the validity of our model.

Finally, the packing fraction at temperature T is deduced from density measurements with the aid of formula:

$$\gamma(T) = \frac{\pi}{6} d^3 \frac{\mathcal{N}}{M} \mu(T) \qquad (17)$$

where $\mathcal{N}$ is the Avogadro number, M the atomic mass and μ the specific mass.

On the other hand, a comparison between experimental and theoretical pair distribution functions involves a Fourier transform of the experimental interference function which introduces truncation and normalization errors. We thus prefer to compare experimental and theoretical structure factors.

3.2. Study of Several Lequid Metals with Different Electronic Structure

3.2.1. Liquid Copper

Using the values $d = 2.56$ Å, $\gamma = 0.656$ and $\sigma = 0.176$ Å or $\nu = 3.9 \cdot 10^{12}$ s^{-1} the liquid copper structure factor at $T = 1150$ °C measured by Breuil and Tourand [15] is fitted within 2% accuracy between K_0

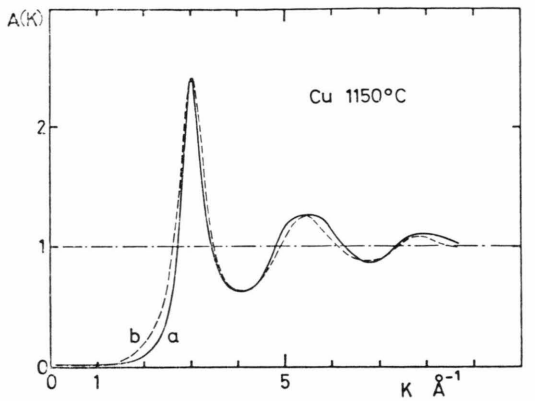

Fig. 5. Copper structure factor: a) from Breuil and Tourand [15], b) from the model.

$= 2$ Å^{-1} and K_{max} (see Figure 5). At $T = 1300$ °C and $T = 1450$ °C, the same agreement is obtained if σ and γ follow respectively relations (16) and (17). However, this temperature range is not wide enough to extrapolate this conclusion to higher temperatures.

3.2.2. Liquid Zinc

For liquid zinc near the melting point ($T = 460$ °C) the values $d = 2.74$ Å, $\gamma = 0.657$ and $\sigma =$

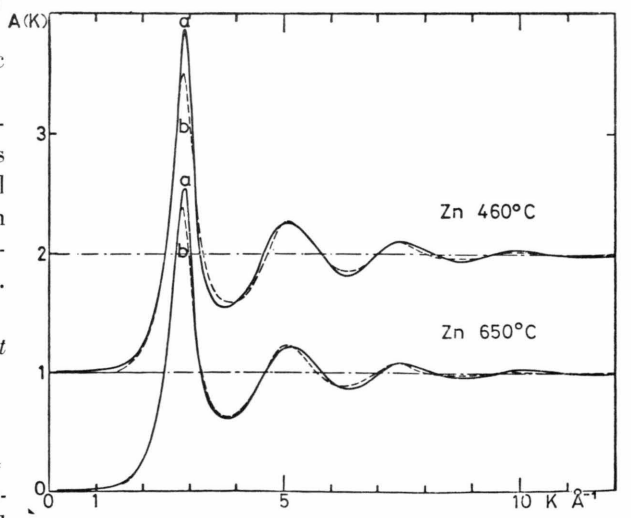

Fig. 6. Zinc structure factor: a) from Knoll [16], b) from the model.

0.165 Å or $\nu = 2.95 \cdot 10^{12}\ s^{-1}$ give a 2% fit to Knoll measurements [16] except for the first $A(K)$ peak (see Fig. 6) which is too low in the present model and agrees better with Enderby results [17]. At $T = 650\ ^\circ C$ and using relations (16) and (17) the agreement with Knoll's $A(K)$ first peak improves.

3.2.3 Liquid Lanthanum, Cerium and Praseodymium

The first measurements of Bellissent, Breuil and Tourand [18, 19] on liquid rare earths have shown that the structure factor of these elements exhibit a low first peak and strong oscillation damping. However, some discrepancies between their results and the present model still remain on the first peak shape and on the first minimum and second peak intensities. These difficulties have been overcome by the more recent measurements of Enderby and Nguyen [20] which our model can fit with 2% precision between $K_0 = 1.3\ Å^{-1}$ and $K_{max} \cong 7\ Å^{-1}$ and using the values $d = 3.74$ Å, $\gamma = 0.705$ and $\sigma = 0.325$ Å or $\nu = 1.34 \cdot 10^{12}\ s^{-1}$ (see Figure 7). The special rare earth behaviour is thus shown to be due to a very soft interaction potential.

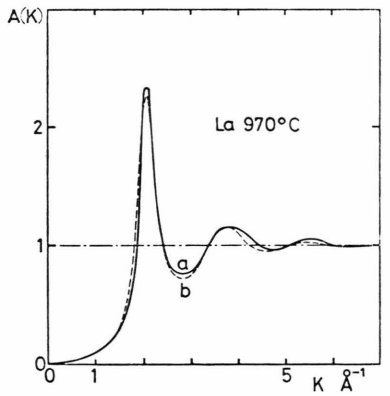

Fig. 7. Lanthanum structure factor: a) from Enderby [20] and Nguyen, b) from the model.

3.3. Temperature Measurements on Liquid Rubidium

Measurements near the melting point ($T = 320\ ^\circ K$) have been performed by Howells and Copley [21]. They may be interpreted with 2% accuracy using the values $d = 5.03$ Å, $\gamma = 0.74$ and $\sigma = 0.365$ Å or $\nu = 0.77 \cdot 10^{12}\ s^{-1}$, except for the first $A(K)$ peak which is again too low in the model.

The first peak discrepancy disappears at higher temperatures. This result may be attributed to the rough treatment of the long range part of the interatomic potential which is responsible for the small K behaviour of the structure factor or to a structural departure from the random hard sphere network at low temperature where the liquid may retain some crystalline features involving more sixfold local symmetry axes. On the other hand, temperature measurements of the structure factor first peak between $K = 1$ and $K = 2.3\ Å^{-1}$ and over a temperature range: $450\ ^\circ K < T < 1400\ ^\circ K$ have recently been performed [22] which provide a good test for relation (16). Figure 8 shows that the agreement between theoretical and experimental maximum intensities is excellent if one uses the value $d = 5.146$ Å. The shift of the first peak due to the liquid dilatation obviously cannot be described with the present model since it corresponds to anharmonic effects. The slight discrepancy in the first peak wings should be reduced by resolution corrections [23].

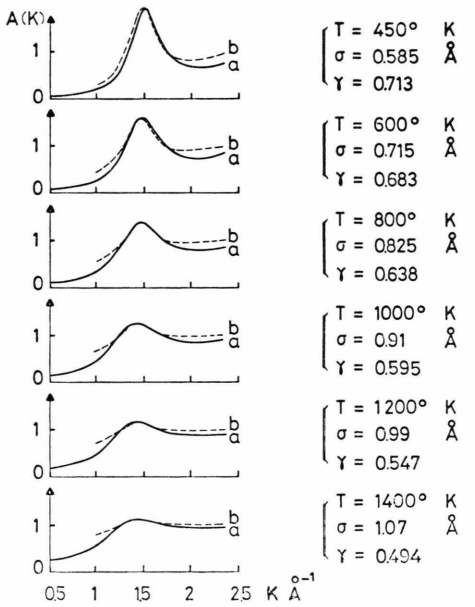

Fig. 8. Temperature variation of the rubidium structure factor first peak: a) from Block, Suck, Freyland, Hensel, and Gläser [22], b) from the model.

Conclusion

Differences between liquid metal diffraction patterns have been interpreted by means of an harmonic approximation where atoms vibrate around

the equilibrium positions of a universal random hard sphere network (which incidentally should be a good initial configuration for M.C. and M.D. calculations). This model depends on three parameters of which the only adjustable one is the vibration frequency which is about one half of the Debye frequency of the corresponding crystalline phase. The atomic diameter is deduced from the position of the structure factor first peak and turns out to be equal to the Goldschmidt diameter. The temperature variation of the packing fraction is attributed to the presence of a variable number of randomly distributed atomic holes and is deduced from density measurements. This simple theory can fit fairly well the most recent structure factor determinations on a wide variety of liquid metals. It is thus shown that very accurate experimental values are needed in order to discriminate between different models and in particular to prove the existence of more than two body forces.

Acknowledgements

Numerical calculations were performed on the I.L.L. PDP10 computer and greatly shortened by Dr. M. Lesourne's word packing programs. Thanks are also due to all the operators and computer staff for their kind cooperation.

During the writing of this paper, suggestions from Drs. P. Chieux and W. S. Howells were very helpful and greatly appreciated.

I am also indebted to Dr. W. Knoll and J. B. Suck for many useful discussions.

[1] J. D. Bernal, Proc. Roy. Soc. London **A 280,** 299 [1964].
[2] J. L. Finney, Proc. Roy. Soc. London **A 319,** 479 [1970].
[3] N. Metropolis, A. W. Rosenbluth, M. N. Rosenbluth, and A. H. Teller, J. Chem. Phys. **21,** 1087 [1953].
[4] B. J. Alder and T. E. Wainwright, J. Chem. Phys. **31,** 459 [1959].
[5] L. Verlet, Phys. Rev. **165,** 201 [1968].
[6] A. Rahman, Phys. Rev. **136,** A 405 [1964].
[7] W. Hoover, S. Gray, and K. Johnson, J. Chem. Phys. **55,** 1128 [1971].
[8] J. F. Sadoc, J. Dixmier, and A. Guinier, J. of Non Cryst. Sol. **12,** 46 [1973].
[9] G. Fournet, Bul. Soc. Franc. Min. **74,** 37 [1951].
[10] A. Guinier, Théorie et Technique de la Radiocristallographie, Dunod [1964].
[11] J. P. Hansen and D. Schiff, Mol. Phys. **25,** 1281 [1973].
[12] J. P. Hansen, Phys. Rev. **A 2,** 221 [1970].
[13] P. Hicter, F. Durand, and E. Bonnier, J. de Chimie Physique **68,** 804 [1971].
[14] H. Ruppersberg and P. Hicter, Conference on the Properties of Liquid Metals Tokyo 577 [1972].
[15] M. Breuil and G. Tourand, J. Phys. Chem. Sol. **31,** 549 [1970].
[16] W. Knoll, to be published in the proceedings of the 3rd international conference on liquid metals (Bristol 1976).
[17] J. E. Enderby, private communication.
[18] M. Breuil and G. Tourand, Phys. Lett. **29 A,** 506 [1969].
[19] R. Bellissent and G. Tourand, J. Phys. **36,** 97 [1975].
[20] J. E. Enderby and V. T. Nguyen, J. Phys. C. **8,** L112 [1975].
[21] W. S. Howells and J. R. D. Copley, private communication.
[22] R. Block, J. B. Suck, W. Freyland, F. Hensel, and W. Gläser, to be published in the proceedings of the 3rd international conference on liquid metals (Bristol 1976), and Ber. Bunsenges. **80,** 718 [1976].
[23] J. B. Suck, private communication.
[24] International tables for X-ray crystallography, Vol. III.
[25] J. Smithells, Metals reference book Vol. I.